

ENVIRONMENTAL PROTECTION

UDC 539.16.004.8

BASALT-BASED GLASS MATERIALS FOR IMMOBILIZING MEDIUM-LEVEL WASTE

O. V. Tolstova,¹ T. N. Lashchenova,¹ and S. V. Stefanovskii¹Translated from *Steklo i Keramika*, No. 6, pp. 28–31, June, 2002.

Samples based on liquid radioactive waste (LRW) and basalt with a weight content of LRW up to 30% are synthesized at temperatures of 1200–1400°C. The obtained materials, in addition to the vitreous phase, contain crystalline phases (clinopyroxene of the aegirite-hedenbergite composition and spinel). The glass materials synthesized from basalt and radioactive slag contain gehlenite and silicophosphates, and as the basalt content increases, augite (aegirite-hedenbergite) is synthesized as well. Crystalline phases capable of including radionuclides are formed in the synthesized materials, which decreases their leaching rate.

In vitrification of radioactive waste (RAW) it is very important to select adequate additives, among which the most suitable appear to be industrial waste and mineral rocks, in particular, basalt. Frequent experiments in vitrification of liquid and solid RAW, such as ash residue, including plutonium-bearing ash residue and superfluuous armament plutonium, using basalt were repeatedly carried out in different countries [1–5]. Moreover, there are many studies on the synthesis of basalt-like materials for immobilization of RAW [6]. The present study considers the materials produced under vitrification of liquid and solid medium-level RAW in the presence of basalt at the Radon Company.

Liquid RAW accumulated at the specialized facilities of the Radon company and generated at nuclear power plants (NPP) using nuclear reactors of the VVER and RBMK types have a complex chemical composition, but the main components are sodium and nitrate ions (60–80%), and in the case of waste from the VVER reactors, hydroxoborate ions as well. The hardness salts (carbonates and hydrocarbonates of calcium and magnesium), the ions of the corrosion products (the iron group elements), phosphate, sulfate, chloride, and fluoride ions are present in smaller quantities. The present study involved vitrification of actual RAW and of simulation waste of a simplified composition. Regarding their radionuclide composition, the RAW mainly contain ^{137}Cs (80–90% of the total activity) and ^{90}Sr (10–15% of the total activity), as well as radionuclides of corrosion products (Cr, Mn, Fe, Co, Ni), rare-earth elements (Zr, Y, La, and Ln

from Ce to Gd) and traces of alpha-emitters (Ra, U, Np, Pu), whose volume activity is 1–3 orders of magnitude lower than that of ^{137}Cs and ^{90}Sr .

The ash residue (slag) from the furnace incinerating solid combustible RAW operated by the MosNPO Radon company has a complex chemical and mineralogical composition and contains up to 20% (here and elsewhere weight content) organic residues and volatile anions (calcination loss). The main activity carriers in this slag are heavy metal radionuclides, including actinides, as well as ^{137}Cs and ^{90}Sr . Radionuclides of corrosion products are present in smaller quantities. The composition of the slag used in the present experiment is as follows (%): 4.7 Na_2O , 4.0 K_2O , 31.0 CaO , 3.0 MgO , 0.3 MnO , 5.0 Al_2O_3 , 2.2 Fe_2O_3 , 1.4 CuO , 21.3 SiO_2 , 0.4 B_2O_3 , 7.0 P_2O_5 , and 0.7 Cl , and 19.0 calcination loss. The share of water-soluble components in the slag was 15.4%, and the moisture was 1.5%.

The fluxing mineral additive added to the RAW was the Kemerovskoe basalt of the following composition (%): 50.5 SiO_2 , 14.8 Al_2O_3 , 14.8 Fe_2O_3 , 1.5 TiO_2 , 5.6 CaO , 3.4 MgO , 0.2 MnO , 3.2 Na_2O , 0.4 K_2O , 0.4 P_2O_5 , and 5.2 the rest.

The batches were prepared by mixing dried salts of liquid RAW or an imitation material and basalt crushed in a porcelain mortar. Batch portions each weighing 10 g were placed in alundum crucibles and heated in a VTP 12/16 resistance furnace to temperatures of 1200–1300°C (to melting) and exposed for 30 min; then a part of the melt was cast on a metal sheet, and the rest was cooled in a switched-off furnace at a rate of about 1 K/min.

¹ Ministry of the Atomic Industry of the RF, Moscow, Russia; Radon Research and Production Association, Moscow, Russia.

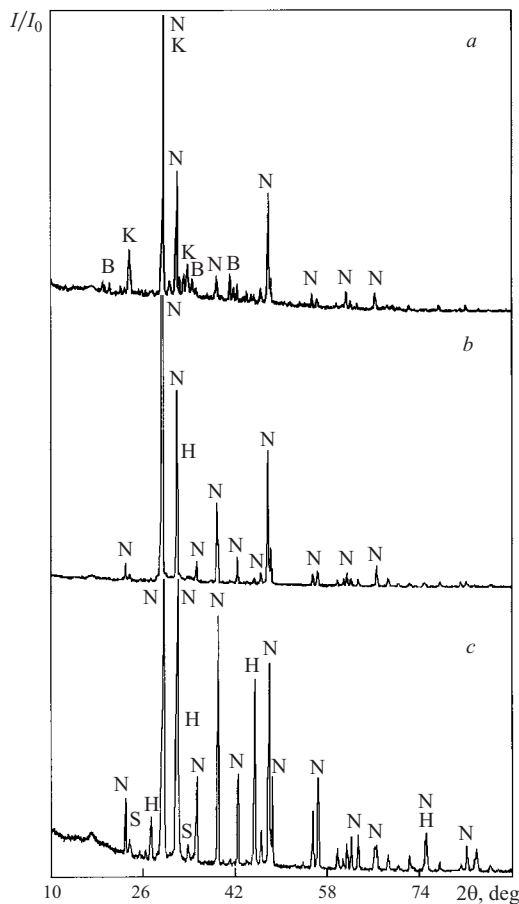


Fig. 1. Diffraction patterns of salt residues of liquid RAW from the Kalinin (a), Kursk (b), and Leningrad (c) nuclear power plants: B) $\text{Na}_2\text{B}_4\text{O}_7 \cdot 5\text{H}_2\text{O}$; H) NaCl ; K) KNO_3 ; N) NaNO_3 ; S) Na_2SO_4 .

The ash residue was cleared of large-size inclusions and crushed in a porcelain mortar to a particle size below 500 μm , mixed with basalt (allowing for calcination loss), and then the obtained batches were heated in a resistance furnace up to their melting (1350 – 1450°C), held for 30 min for homogenization, and cooled in a switched-off furnace at a rate of about 1 K/min.

The resulting samples were studied by x-ray phase analysis (a DRON-4 diffractometer, CuK_α radiation) and scanning electron microscopy with an energy-dispersing system (SEM/EDS) on a JSM-5300 + Link ISIS analytical complex. The rate of leaching the components out of the materials synthesized was determined according to the MSS-1 method (7-day test at 90°C) [7].

The dried residue of liquid RAW is represented by a mixture of salts (Fig. 1). The predominant phase in all mixtures is sodium nitrate (nitratine), whose main reflections are 3.03 – 3.04, 2.80 – 2.81, 2.53, 2.31 – 2.33, 2.12 – 2.13, 1.90 and 1.88 Å. The dry residue of liquid RAW also contains potassium nitrate (the most intense peaks at 3.78, 3.73, 3.03, 2.65, 4.66, 2.76, 2.70, 2.19, 2.16, and 1.95 Å). The RAW generated at the Leningrad and (in smaller quantities) at the

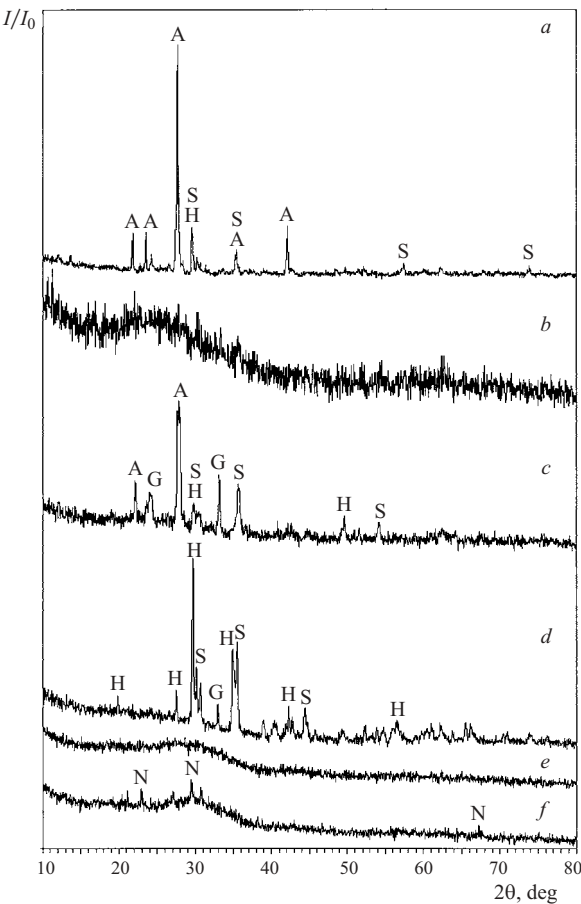


Fig. 2. Diffraction patterns of initial (a), remelted and hardened (b), remelted and slowly cooled (c) basalt, and the products of liquid RAW inclusion in basalt with a RAW oxide content equal to 10% (d), 20% (e), and 30% (f): A) plagioclase; G) gehlenite; H) aegirite-heedenbergite (augite); N) nepheline; S) spinel.

Kursk NPP contains sodium chloride, whose most intense reflections are 2.82, 1.99, 1.63, 3.26, and 1.26 Å (halite). A specific feature of the RAW from the Kalinin NPP (with the VVER reactors) is the presence of borates in the form of $\text{Na}_2\text{B}_4\text{O}_7 \cdot 5\text{H}_2\text{O}$ (tincalconite); its most intense peaks are: 2.92, 4.38, 3.44, 3.00, 2.18 – 2.19, 2.00, and 8.75 Å. Several low-intensity peaks on the diffraction pattern of the dry residue of liquid RAW from the Leningrad NPP (with the RBMK reactors) most probably belong to sodium sulfate.

The main phase in the initial basalt is plagioclase enriched with anorthite ($\text{Ca}, \text{Na})(\text{Si}, \text{Al})_4\text{O}_8$). Most of the reflections in the diffraction patterns belong to it (Fig. 2a). The patterns include spinels (2.53, 3.03 Å and other low-intensity reflections). Pyroxene is presumably present as well. After melting and hardening, a vitreous material is formed on the metal sheet (Fig. 2b). A slow cooling of the melt leads to the crystallization of glass with the formation of plagioclase mainly of the anorthite composition, as well as gehlenite $\text{Ca}_2\text{Al}_2\text{SiO}_7$ and spinels (Fig. 2c). A slow cooling of the melt containing 10% liquid RAW oxides facilitates partial crystallization of glass (Fig. 2d) with the formation of aegirite-

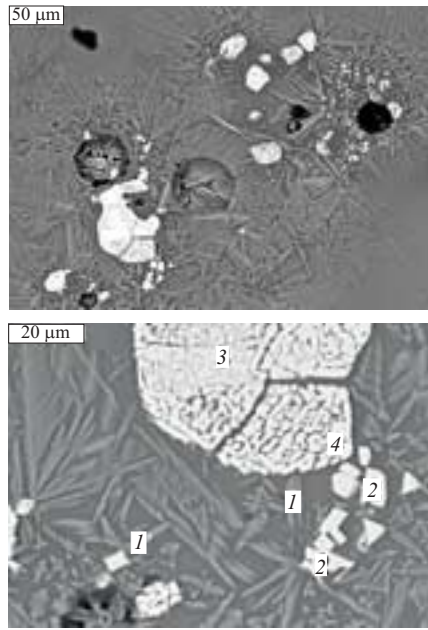


Fig. 3. Scanning electron microscope photos of a glass-ceramic material containing 10% liquid RAW oxides and 90% basalt (top: a general view; bottom: a detail): 1) aegirite-hedenbergite; 2) magnesioferrite; 3) ulvospinel; 4) solid solution of ulvospinel and magnetite-magnesioferrite.

hedenbergite of the composition $(\text{Ca}_{0.6}\text{Na}_{0.36})(\text{Fe}_{0.41}\text{Mg}_{0.38}\text{Ti}_{0.07}\text{Al}_{0.11})(\text{Si}_{1.60}\text{Al}_{0.40})\text{O}_6$ and spinels, which are represented by magnesioferrite $(\text{Mg}_{0.77}\text{Fe}_{0.19}^{2+}\text{Mn}_{0.04}^{2+})(\text{Fe}_{1.86}^{3+}\text{Al}_{0.11}\text{Ti}_{0.03})\text{O}_4$, titanium magnetite $(\text{Fe}_{0.68}^{2+}\text{Mg}_{0.32})(\text{Fe}_{0.68}^{2+}\text{Mg}_{0.32}\text{Fe}_{1.07}^{3+}\text{Fe}_{0.39}^{2+}\text{Ti}_{0.43}\text{Al}_{0.06}\text{Mn}_{0.02})\text{O}_4$, and ulvospinel $\text{Ti}_{1.00}(\text{Fe}_{1.61}^{2+}\text{Mg}_{0.21}\text{Al}_{0.05}\text{Ti}_{0.05}\text{Mn}_{0.01})\text{O}_4$ clearly visible in the electron-microscope photos (Fig. 3).

A melt containing 20% liquid RAW oxides cools in the vitreous state, and neither slow cooling nor even long-time annealing in the temperature range 500–800°C produce crystallization (Fig. 2e). A slowly cooled sample containing 30% liquid RAW oxides (Fig. 2f) contains the nepheline phase, but its content is low (10–20% of the sample volume).

It is unadvisable to increase the content of liquid RAW oxides beyond 30–35%, since this deteriorates the chemical resistance of the samples: as the liquid RAW content increases from 30 to 40%, the ion leaching rate increases from about 10^{-3} to about 1 g/(cm² · day). The reason for this is the destruction of the alumino(boron)silicon-oxygen glass lattice under the effect of the alkali ions, which are present in RAW in large quantities [8].

The ash residue (slag) from a RAW-incinerating furnace consists of glass (the main phase), quartz, a solid solution based on calcium silicate of the composition $(2-3)\text{CaO} \cdot \text{SiO}_2$, and possibly a small impurity of sodium-calcium orthophosphate NaCaPO_4 (Fig. 4a). After melting at a temperature of 1450°C, the vitreous slag contains solid solution $\text{Ca}_3(\text{PO}_4)_2 - \text{Ca}_2\text{SiO}_4$ (Fig. 4b). After 10% basalt is

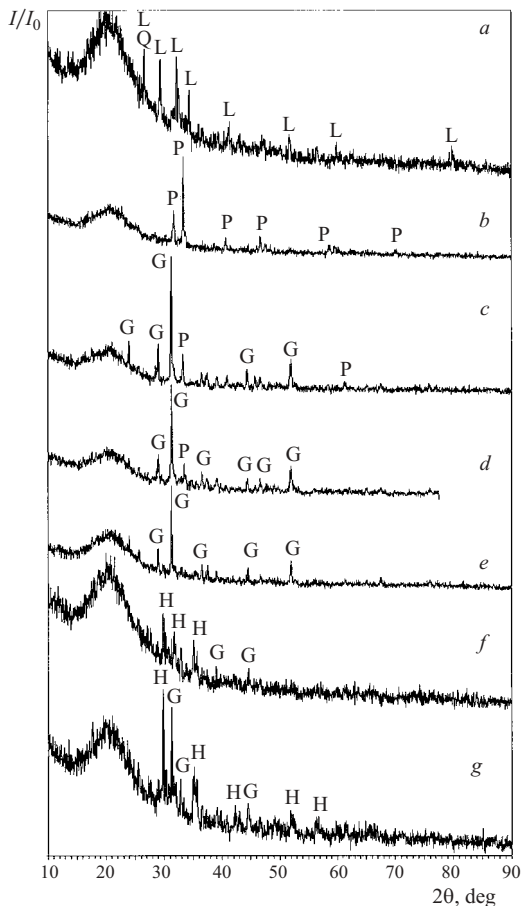


Fig. 4. Diffraction patterns of initial (a) and remelted and slowly cooled (b) slag and of glass slag with the ratio between slag oxides and basalt equal to 90 : 10 (c), 80 : 20 (d), 70 : 30 (e), 60 : 40 (f), and 50 : 50 (g): G) gehlenite; H) aegirite-hedenbergite (augite); L) calcium silicate; P) silicophosphate; Q) quartz.

added, the main phase in the glass ceramics is gehlenite with reflections 2.86 (the most intense), 3.71, 3.07, ~ 2.45 , ~ 2.40 , ~ 2.30 , 2.04, ~ 1.76 , ~ 1.51 , ~ 1.38 , and 1.265 Å (Fig. 4c). There are also relicts of the silicophosphate phase (~ 2.69 , ~ 2.86 , 3.47, ~ 1.95 , and ~ 1.76 Å), whose composition approaches nagel-shmidtite $\text{Ca}_7(\text{PO}_4)_2(\text{SiO}_4)_2$. Similar diffraction patterns are also observed in the samples containing 20 and 30% basalt (Fig. 4d and e). In the sample containing 60% slag and 40% basalt, we find pyroxene of the augite type $\text{Ca}(\text{Mg}, \text{Al}, \text{Fe})\text{Si}_2\text{O}_6$ responsible for the reflections of 2.99 (100%), 3.23, 2.95–2.96, ~ 2.90 , ~ 2.55 , ~ 2.13 , ~ 2.10 , ~ 1.76 Å, and some other less intense reflections. As the basalt content in the samples increases from 10 to 50%, the amount of gehlenite decreases and that of augite increases (Fig. 4c–g). Starting with the composition containing 60% slag and 40% basalt, augite becomes the prevailing phase (Fig. 4f and g).

The formation of these phases is related to a modification of the chemical composition of samples. The initial and the remelted slag have a low content of SiO_2 (35–45%) and a

relatively high quantity of the sum of alkaline (up to 15–20%) and alkaline-earth (20–40%) oxides and may contain up to 20% P_2O_5 (the rest consist of oxides of aluminum, iron, other transition metals, and metal impurities). Virtually all phosphor and a small part of silicon is segregated as an alkaline-earth silicophosphate phase. The remaining vitreous phase is enriched with alkalis, silica, and oxides of transition metals and aluminum. On adding basalt, the concentrations of silica and alumina in the materials monotonically grow, and the concentrations of alkalis and phosphates decrease. This facilitates the crystallization of the aluminosilicate phase (gehlenite). With a basalt content of more than 30%, the quantity of the silicophosphate phase becomes negligible, and the formation of pyroxene, which is the phase typical of basalt, starts along with gehlenite. A further increase in the acidity of the melts stimulates the crystallization of plagioclase, which constitutes the main phase of basalt.

The emerging phases are capable of including radionuclides. Such phases in samples with liquid RAW oxides are pyroxene (aegirite-hedenbergite), nepheline, and spinels. The first two phases may include radionuclides of alkaline metals and elements of the iron group. Spinels can be matrix phases for radionuclides of the corrosion products (Ti, Cr, Mn, Fe, Co, Ni). In samples with solid RAW oxides, silicophosphates incorporate actinides, radionuclides of rare-earth elements, and ^{90}Sr , whereas aluminosilicates incorporate radionuclides of alkaline metals and the iron group elements (corrosion products).

The rate of leaching of radionuclides out of glass slag, which was determined according to the MCC-1 method, is

equal to about 10^{-3} g/(cm² · day), which is lower than the rate of leaching out of traditional borosilicate glasses used to immobilize medium-active waste.

The authors acknowledge the help of B. S. Nikonor (IGEM Institute, Russian Academy of Sciences) in performing the electron microscope studies of the samples.

REFERENCES

1. Ya. Spidl and Ya. Ralkova, "Solidification of radioactive waste by melting into basalt," *Atom. Energ.*, **21**(4), 285–289 (1966).
2. I. A. Sobolev, S. V. Stefanovskii, F. A. Livanov, et al., *Fiz.-Khim. Obrab. Mater.*, Nos. 4–5, 150–160 (1994).
3. M.-J. Lebeau and M. Girod, "Incorporation of simulated nuclear ashes in basalt: an experimental investigation," *Am. Ceram. Soc. Bull.*, **66**(11), 1640–1646 (1987).
4. M. J. Kupfer, W. W. Schulz, C. W. Hobbs, and J. E. Mendel, "Glass forms for alpha waste management," *AIChE Symp. Ser.*, **72**(154), 90–97 (1976).
5. Y. I. Matyunin, S. V. Yudintsev, and L. J. Jardine, "Immobilization of plutonium-containing waste into borobasalt, pyroxene and andradite mineral-like compositions," in: *Plutonium Future, The Scie. Conf. Trans., Santa Fe* (2000), p. 179.
6. J. M. Welch, P. V. Kelsey, S. P. Henslee, et al., "Iron-enriched basalt for containment of nuclear wastes," *Mat. Res. Soc. Symp. Proc.*, **6**, 23–30 (1982).
7. *Nuclear Waste Materials Handbook (Test Methods): DC. Report DOE/TIC-11400*, Washington (1981).
8. S. V. Stefanovskii, "EPR and IR spectroscopic study of the structure of borosilicate glasses for immobilization of radioactive waste," *Radiokhimiya*, No. 3, 214–222 (1992).